AIAA 81-1981R

An Iterative Method for Predicting Turbofan Inlet Acoustics

S. J. Horowitz,* R. K. Sigman,† and B. T. Zinn‡
Georgia Institute of Technology, Atlanta, Georgia

A new iterative solution technique for predicting the sound field radiated from a turbofan inlet is presented. The sound field is divided into two regions; the sound field within the inlet which is computed using the finite element method and the radiation field outside the inlet which is calculated using an integral solution technique. A "unified" solution is obtained by matching the finite element and integral solutions at the interface between the interior and exterior regions. The applicability of the iterative technique is demonstrated by considering several simple cases for which exact or "classical" solutions for the sound field are available. These examples show that the proper solution is obtained within five iterations. The overall accuracy of the method is demonstrated by comparison with experimental data.

Introduction

GROWING concern in recent years over the rise in noise pollution, especially that caused by turbofan engines, has created considerable interest in developing methods for predicting the acoustic properties for these engines. The two major sources of turbofan engine noise are the externally generated noise produced by the jet exhaust and the internally generated noise due to the rotating turbomachinery, turbofan blades, and combustion processes. The noise due to jet exhaust has become less intense due to the use of high bypass ratio turbofan engines which have a reduced jet velocity over earlier low bypass ratio engines. This, in turn, has made the noise produced by the turbofan more apparent. In an attempt to reduce the turbofan noise, much effort has been expended in the development of acoustic liners for these engine inlets. Unfortunately, due to the lack of analytical methods for such development, most of the design work for these liners has been performed by costly cut and try methods. For this reason, analytical methods are needed to equip the designer with the tools necessary for the job of designing quieter efficient turbofan inlets.

As the first step in a theoretical approach to reducing the amount of noise that will reach an observer, whether it be a passenger in the aircraft or an observer on the ground, an analytical procedure for predicting the acoustic field of the engine must be developed. This analysis should include the effects produced by short inlet ducts with varying geometry and lined inlet walls. To date, no such analytical method for predicting the entire sound field exists. This paper describes a general approach for calculating the acoustic field of a turbofan inlet. The approach is not restricted to any particular computational schemes. Thus, many of the analytical approaches presently used in duct acoustics can be extended to provide a realistic description of the entire sound field.

Consider the somewhat idealized inlet shown in Fig. 1. Noise produced within the engine propagates down the inlet duct and radiates out to the surrounding environment. The rear portion of the inlet is replaced by an ellipsoidal termination since the geometry of this region has very little effect on the sound radiated from the inlet. For reasons to be discussed later, it is convenient to separate the acoustic field into two regions: the "interior" region within the inlet duct and the "exterior" region consisting of the unbounded region surrounding the inlet. It should be emphasized that this is a separation of convenience and the correct acoustic field must be continuous across the interface. However, most analyses of the acoustic field to date have considered the acoustic properties of these two regions separately without attempting to match the solutions at the interface and obtain a continuous description of the acoustic field.

One classical example of this approach is the work of Tyler and Sofrin.[1] In this analysis, the inlet was taken to be a straight duct with the separation of the acoustic field coinciding with the end of the duct (i.e., the inlet entrance of Fig. 1). For the interior problem, it was assumed that there was no reflection of sound from the end of the inlet, and the method of separation of variables was used to obtain exact solutions. This "exact" solution within the duct predicts the acoustic pressure and velocity at the inlet entrance. This pressure at the entrance is used to construct a simple radiation model for calculating the sound field in the exterior region. This radiation model is based on the far field approximation of a piston in an infinite baffle. However, the impedance of the piston used in the exterior region differs from the no reflection impedance assumed for the interior solutions. This indicates a discontinuity in the acoustic velocity at the entrance of the duct. No attempt is made by Tyler and Sofrin to remove this discontinuity.

The assumption of no reflection at the exit used by Tyler and Sofrin provides a reasonable approximation which is used to derive the inlet entrance plane boundary condition. Rice[2] has argued that this approximation is valid if the frequency is above the cutoff frequency of the mode under consideration. Unfortunately, many computational approaches (finite element, finite difference) do not separate the acoustic waves into individual modes. In these cases, the correct boundary condition for no reflection of plane waves will produce a reflection of higher-order radial modes.

One alternative to the no-reflection impedance is the use of experimentally determined values of the exit impedance. In their finite element approach, Tag and Lumsdaine[3] used an empirical formula based on previous experimental results.[4] This approach provides the correct reflection for a single mode, but as in the no-reflection case, unless a mode matching approach is used, any additional modes present in the duct will not be reflected correctly.

Submitted Oct. 16, 1981; presented as Paper 81-1981 at the AIAA Seventh Aeroacoustics Conference, Palo Alto, Calif., Oct. 21-23, 1981; revision received April 15, 1982.

*Graduate Research Assistant, School of Aerospace Engineering; presently Associate Scientist, Lockheed-Georgia Company, Marietta, Ga. Member AIAA.

†Senior Research Engineer, School of Aerospace Engineering. Member AIAA.

‡Regents' Professor, School of Aerospace Engineering. Associate Fellow AIAA.

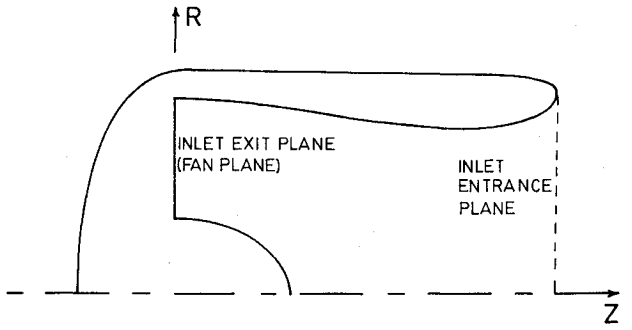

Fig. 1 Idealized inlet geometry.

Although to date the acoustic fields predicted by such field separation approaches are discontinuous, the approach is still valid. Baumeister[5] has argued that the two regions are usually not strongly coupled, and the discontinuities can be removed by repeated calculation of the interior and exterior acoustic regions until the two solutions match at the interface.

Although it is possible to develop a single analytical approach for the entire acoustic field, the separation approach is convenient for several reasons. Since the noise reduction techniques (e.g., sonic inlet, acoustic liners), are applied to the interior of the inlet, the mathematical difficulties encountered in the interior region are usually more severe than those encountered in the exterior region. Thus, computation time can be reduced by using different analytical approaches in the two regions. Further computation time can be saved in optimization studies by repeating calculations only in the interior region until nearly optimum values of parameters (e.g., liner impedance values) are obtained. Final values of the optimum parameters are obtained by matching the interior and exterior regions.

Because of the nature of the regions, analytical approaches to the solution of the acoustic equations in the interior (finite) and exterior (infinite) regions are fundamentally different. Within the interior of the inlet, computational approaches based on numerical quadrature of the governing differential equation, such as finite element methods,[6-8] finite difference methods,[9,10] and various mode matching techniques[11,12] have been developed. In the infinite exterior region, the so called integral technique,[13-15] which employs Green's theorem to transform the volume integral of the acoustic equation to a lower-order integral over the surface of the inlet, has been employed successfully. Although the finite element, finite difference, and mode matching techniques are in general restricted to use in finite regions, the integral technique can be used to describe the entire acoustic field.[13] However, as previously noted, use of the integral technique to describe the entire continuous acoustic field is not always computationally efficient. Thus, it is desirable to separate the acoustic field into two regions and apply the appropriate mathematical tools to each region.

The purpose of this paper is to show that using simple iteration procedures, acoustic solutions for the interior and exterior problems can be forced to match at the interface and produce a continuous description of the acoustic field. Solutions for the interior region are obtained using finite element codes described in previous papers.[6,7,16] The integral technique of Meyer[13,14,17] is used to obtain solutions in the exterior region. Boundary conditions can be prescribed on all boundaries of the interior and exterior regions with the exception of the interface which is an artificial boundary. Using an iterative scheme to be described later, the impedance and potential are alternately prescribed and calculated at the interface in the interior and exterior regions. Calculations are repeated until the solutions match at the interface.

It should be noted that the iteration procedure can be avoided by coupling the two procedures together.[18] This approach has two disadvantages; first, by adding the square matrix produced by the integral technique to the banded matrix of the finite element method, the computational efficiency of the solution of the banded matrix is destroyed. More importantly, each procedure, finite element or integral technique uses nearly the entire storage capacity of the Georgia Institute of Technology CDC Cyber 70/74. Thus, if computing accuracy is to be maintained, a computer with larger memory must be used.

Problem Formulation

Formulation of the problem involves specification of the governing equations and boundary conditions, a description of the geometry, and an outline of the mathematical approach.

Governing Equations

Consider a stagnant, inviscid, non-heat conducting, homogeneous gas with pressure p_0, density ρ_0, and sound speed c_0. The small acoustic disturbances to the quiescent gas have pressure p', density ρ', and velocity q', which are nondimensionalized by $\rho_0 c_0^2$, ρ_0, and c_0, respectively. All lengths are nondimensionalized by the duct diameter at the fan plane d_0. All disturbances are assumed to be isentropic and irrotational, so that a velocity potential can be defined by

$$q' = \nabla \varphi' \tag{1}$$

All disturbances are assumed to vary sinusoidally with time

$$\varphi'(r,t) = \varphi(r) e^{-i\omega t} \tag{2}$$

where, in general, any time-dependent primed quantity is equal to the equivalent unprimed quantity multiplied by $e^{-i\omega t}$. Under these conditions, the continuity, momentum, and energy equations can be combined to give the well-known Helmholtz equation

$$\nabla^2 \varphi + k^2 \varphi = 0 \tag{3}$$

where

$$k = \omega d_0 / c_0$$

Equation (3) is written in a cylindrical coordinate system (r,θ,z) with the z axis coinciding with the duct centerline (see Fig. 1). The original formulation of the finite element method[6] and the integral technique[14] used in this paper included sinusoidal variation in the azimuthal direction (i.e., spinning waves). For simplicity, this paper will consider only cases with cylindrical symmetry (i.e, $\partial/\partial\theta = 0$). The extension to spinning waves is straightforward. Thus, for cylindrically symmetric acoustic propagation, Eq. (3) becomes

$$\frac{\partial^2 \varphi}{\partial r^2} + \frac{1}{r}\frac{\partial \varphi}{\partial r} + \frac{\partial^2 \varphi}{\partial z^2} + k^2 \varphi = 0 \tag{4}$$

The acoustic pressure is related to the acoustic potential through the momentum equation

$$p = ik\varphi \tag{5}$$

Boundary Conditions

To complete the problem formulation, the boundary conditions for the problem must be specified. The geometry of an inlet is shown in Fig. 1. In order to specifically prescribe the boundary conditions, the region in Fig. 1 is divided into a finite interior region and an infinite exterior region as shown in Fig. 2.

Interior Region

As shown in Fig. 2, the boundaries of the interior region are: the upper duct wall, the inlet exit plane, the centerbody wall (if present) and axis of symmetry, and the inlet entrance

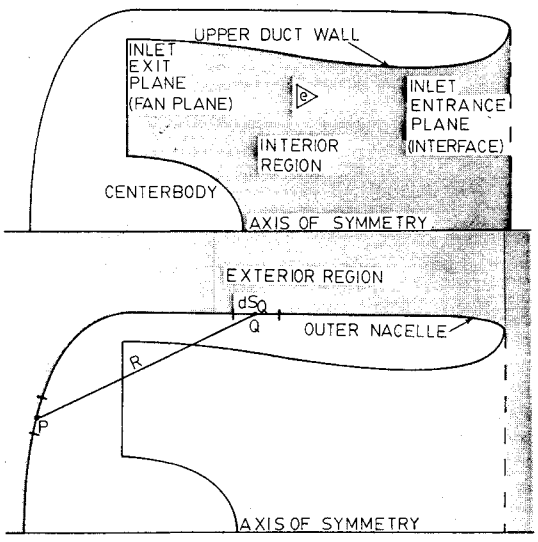

Fig. 2 Geometry of interior and exterior regions.

plane. As discussed in Ref. 6, the finite element formulation requires specification of the acoustic velocity component normal to each of the boundaries (i.e., $\partial\varphi/\partial n$). Along the upper duct wall, the hard wall boundary condition

$$\partial\varphi/\partial n = 0 \tag{6}$$

or the impedance boundary condition for a point reacting liner

$$\frac{\partial\varphi}{\partial n} = \frac{ik\varphi}{Z_\ell} \tag{7}$$

is specified where appropriate. On the centerbody or axis of symmetry, Eq. (6) again applies. The inlet exit plane is the interface between the inlet and the turbofan engine and is, therefore, the location where the noise enters the duct. As previously noted, this paper will consider only axially symmetric acoustic disturbances. Thus, the noise source at the inlet exit is given by

$$\frac{\partial\varphi}{\partial n} = -f(r) \tag{8}$$

For axially symmetric plane wave excitation, $f(r)$ equals a constant. The inlet entrance plane represents the artificial interface which separates the interior and exterior regions. On the interface, the normal acoustic velocity and acoustic pressure are related by an impedance condition

$$Z_{Ii} = p \Big/ \frac{\partial\varphi}{\partial n} \tag{9}$$

where the subscript i represents the "interior" value of the impedance. Since the value of Z_{Ii} is not known a priori, an iteration scheme is used to determine the correct value of Z_{Ii}.

Exterior Region

The boundaries of the outer region consist of the axis of symmetry, the inlet entrance plane (or interface), and the outer nacelle wall. On the axis of symmetry and the outer nacelle wall, Eq. (6) holds. At the inlet entrance plane, an axially symmetric acoustic potential is introduced

$$\varphi(r) = g(r) \tag{10}$$

As will be described later, values of $g(r)$ are obtained from the internal solution and change with each iteration.

Finally, in the proper physical description of the problem, no sound would be emitted before the engine was started at time t_0, and thus no disturbances would exist beyond $R = c_0(t - t_0)$. In the stationary formulation, this restriction is stated by the Sommerfeld radiation conditions

$$|\varphi R| < K \text{ as } R \to \infty \tag{11}$$

where K is a finite number and

$$R\left(\frac{\partial\varphi}{\partial R} - ik\omega\right) \to 0 \text{ as } R \to \infty \tag{12}$$

where

$$R = \sqrt{z^2 + r^2} \tag{13}$$

In the integral technique, these conditions are met by choosing the Green's functions which satisfy these conditions.

Iteration Scheme

With the form of the boundary conditions specified, it is possible to formulate a simple iterative scheme. Specification of a physical problem involves a description of the inlet geometry, specification of the location and impedance values of acoustic liners (if present), and the nature of the sound source [i.e., $f(r)$]. With these conditions specified, all boundary conditions are known with the exception of Z_{Ii} in the interior region and $g(r)$ in the exterior region. In order to match the two regions, a simple iterative procedure based on the method of successive substitution can be formulated as follows.

1) Employing the no-reflection impedance condition ($Z_{Ii} = 1.0$), use the finite element method to obtain a solution within the interior region. From this solution compute the acoustic potential at the interface.

2) Let the acoustic potential at the interface as computed in step 1 equal $g(r)$. Use the integral technique to compute the exterior field. From the exterior solution, compute the impedance at the entrance plane (i.e., Z_{Ie}) where the subscript e denotes the external impedance at the interface.

3) If Z_{Ie} is not equal to Z_{Ii}, set Z_{Ii} equal to Z_{Ie} and repeat the solution of the interior region using the finite element method and obtain a new acoustic potential, $g(r)$, at the interface.

4) Using the $g(r)$ calculated in step 3, repeat the solution of the exterior region using the integral technique and obtain a new interface impedance Z_{Ie}.

5) Repeat steps 3 and 4 as necessary until the impedance used in step 3, Z_{Ii}, agrees with the impedance calculated in step 4, Z_{Ie}, within a specified tolerance.

Computational Methods

The finite element method and the integral technique used in this paper are described in detail elsewhere.[6,7,13,14,16,17] For completeness, a brief description of each method is presented in this section. It should be noted that computational schemes such as finite difference methods[9,10] or other integral approaches[15] could also be used in this iteration scheme.

Finite Element Method

Solution of Eq. (4) by the finite element method (FEM) requires a reformulation of the differential equation as an integral equation. It has been shown by Zienkiewicz[19] that a variational principle can be obtained for the Helmholtz equation. The variational principle represents the preferred integral equation for use in the FEM. Since the original formulation of the FEM[6] considered the acoustics of a moving medium for which no variational principle has been determined, a Galerkin approach was employed. Since the ultimate goal of this research is to develop a "total field"

approach for inlets in flight, the Galerkin approach will be retained. This allows for the use of the original finite element computer codes without changes. Following Ref. 6, Galerkin's form of the method of weighted residuals can be written as

$$\sum_{e=1}^{E} \int\int N_m^e \left\{ \frac{\partial^2 \varphi}{\partial r^2} + \frac{1}{r}\frac{\partial \varphi}{\partial r} + \frac{\partial^2 \varphi}{\partial z^2} + k^2 \varphi \right\} r\,dr\,dz = 0$$

$$m = 1,2,\ldots M \qquad (14)$$

Where N_m^e is the weighting function for node m, over element e. E is the total number of nodes for element e.

As described by Sigman et al.,[6] the region (see Fig. 2) is subdivided into triangular elements, and linear interpolating functions (weighting functions) are employed.

Integral Technique

The integral technique developed by Meyer et al.[13] is normally used to describe the entire acoustic field of a turbofan inlet. As previously noted, this paper uses the integral approach only in the exterior region shown in Fig. 2.

As shown by Meyer et al.,[13] Green's theorem can be used to rewrite Eq. (3) in the following integral form.

$$\int_0^l \varphi(Q)\{K_1(P,Q) + K_2(P,Q)\}\,dS_Q - \varphi(P)\int_0^l \{F_1(P,Q) + F_2(P,Q)\}\,dS_Q - \int_0^l \frac{\partial \varphi(Q)}{\partial n}\{I_1(P,Q) + I_2(P,Q)\}\,dS_Q = 2\pi\left\{\varphi(P) + \frac{i}{k}\frac{\partial \varphi(P)}{\partial n}\right\} \qquad (15)$$

As shown in Fig. 2, P is a specific point on the body and Q the integration point that traverses the body surface. The functions K_1, K_2, F_1, F_2, I_1, and I_2 are circumferential integrals that are functions of the body geometry and the Green's function. For example,

$$K_1(P,Q) = 2\int_0^{\pi} \frac{\partial G(P,Q)}{\partial n_Q}\,d\theta_Q \qquad (16)$$

Green's function, $G(P,Q)$ is

$$G(P,Q) = \frac{e^{ikR(P,Q)}}{R(P,Q)} \qquad (17)$$

where

$$R(P,Q) = \sqrt{(z_P - z_Q)^2 + (r_P - r_Q)^2} \qquad (18)$$

Note that Eq. (17) satisfies the Sommerfeld conditions [i.e., Eqs. (11) and (12)].

Equation (15) is reduced to a set of N linear algebraic equations by subdividing the boundary in Fig. 2 into N segments. The point P is fixed at the midpoint of a segment and the required integrations are performed over the boundary to produce an algebraic equation. Note that the normal derivative of the acoustic potential is known on the boundary, being equal to zero on the hard walled portion and given by $g(r)$ at the entrance plane. By letting P be the midpoint of each of the N segments, N algebraic equations are obtained. The square matrix representing the N algebraic equations is inverted using standard matrix methods.

Results

Computed results are presented for a wide variety of cases. First the convergence and the accuracy of the approach are demonstrated for a simple acoustic problem for which an exact solution is known. Next, exit impedances are calculated for a semi-infinite straight duct and compared with classical results. Finally, the acoustic field of a NASA QCSEE inlet is computed and compared with experiment.

Oscillating Sphere

Consider a sphere of diameter 1.0 oscillating in free space as shown in Fig. 3. The velocity on the sphere is given by

$$\frac{\partial \varphi}{\partial n} = \frac{e^{ikR}}{R}\left(ik - \frac{1}{R}\right) \qquad (19)$$

where the time dependence of $e^{-i\omega t}$ has been assumed. A solution of Eq. (4) subject to the boundary condition Eq. (19) is

$$\varphi = e^{ikR}/R \qquad (20)$$

where R is the distance from the origin defined in Eq. (13). Equation (20) represents a unit point source located at the origin. Note that since the point source is not located within the region of interest, no singularities appear in the acoustic field.

As shown in Fig. 3, the infinite domain is separated into interior and exterior regions by a sphere of radius 1.0. The interior region, $0.5 \le R \le 1.0$, was subdivided into 224 triangular elements with 264 nodal points. The boundary condition on the sphere $R = 0.5$ is given by Eq. (19) and for the initial FEM calculations, an impedance $Z_{Ii} = 1.0$ was used on the interface $R = 1.0$. The FEM calculations produce an acoustic potential distribution on the outer sphere. The boundary $R = 1.0$ is subdivided into 64 segments for the integral technique and the acoustic potential distribution calculated by the FEM is prescribed at each midpoint. The iteration scheme described in a previous section was used to match the acoustic solutions at the interface.

Since the exact solution for this problem is known, the convergence of the iterations can be determined by computing a mean absolute difference between the computed potential and the exact potential at each finite element nodal point

$$\text{mean error} = \frac{1}{N}\sum_{i=1}^{N} |\varphi_{i\ \text{comp}} - \varphi_{i\ \text{exact}}| \qquad (21)$$

The mean error is shown in Fig. 4 for three iterations for a sphere oscillating at $k = 1.0$. It is clear that further iterations will not produce any improvement, i.e., the computational procedures have about a 2% error. In fact, convergence is obtained after the first iteration.

Due to the extremely rapid convergence observed in this case, a more demanding case was formulated. The previously posed problem was again considered, but a poor initial estimate of the impedance at the interface was used. As shown in Fig. 5, an impedance of $Z_{Ii} = 1.0$ was applied in the "front" part of the sphere ($R = 1.0$) and $Z_{Ii} = 3.0$ was applied over the remainder of the sphere. As shown in Fig. 6, while the initial mean error was extremely large, convergence was obtained in three iterations.

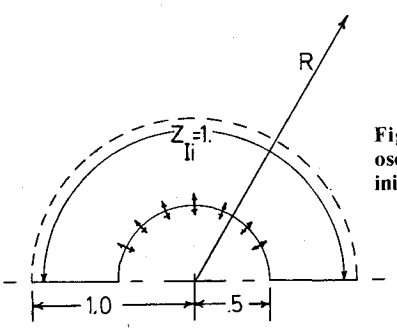

Fig. 3 Geometry of oscillating sphere with good initial impedance estimate.

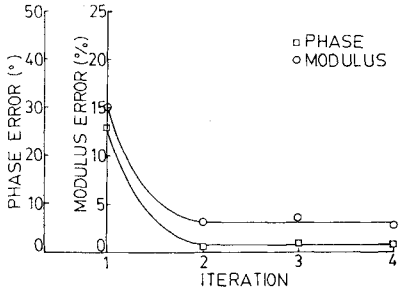

Fig. 4 Mean error between exact solution and FEM calculation after each iteration for good initial impedance estimate.

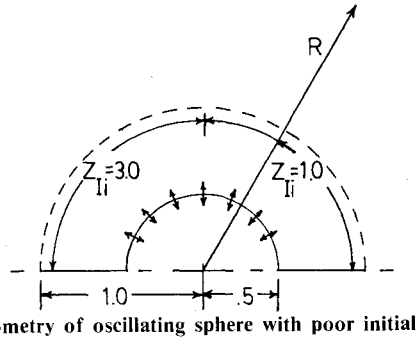

Fig. 5 Geometry of oscillating sphere with poor initial impedance estimate.

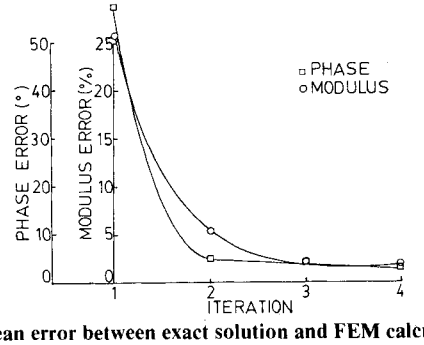

Fig. 6 Mean error between exact solution and FEM calculation after each iteration for poor initial impedance estimate.

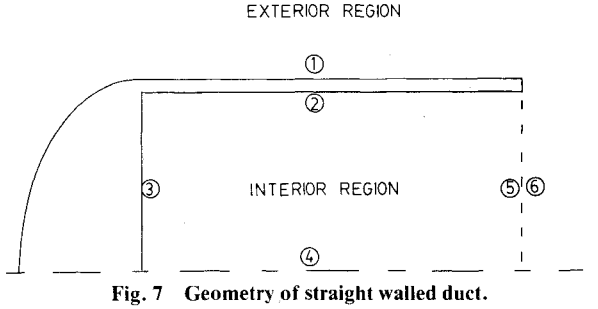

Fig. 7 Geometry of straight walled duct.

Plane Wave Propagation in a Straight Duct

This example represents a simple model for a turbofan inlet. The geometry of the inlet is shown in Fig. 7.

Boundary 3 represents the inlet exit plane where the engine noise enters the inlet duct. On boundary 3, an axially symmetric plane wave sound source is prescribed.

$$\frac{\partial \varphi}{\partial n} = -\frac{\partial \varphi}{\partial z} = -1.0 \tag{22}$$

In the interior region shown in Fig. 7, the boundary conditions on surfaces 2 and 4 are given by Eq. (6). For the initial

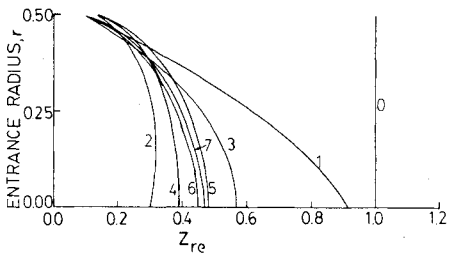

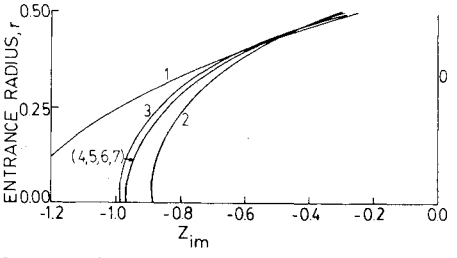

Fig. 8 Iterated exit impedance for a straight circular duct, $k = 2.0$.

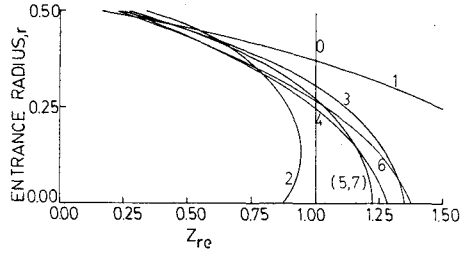

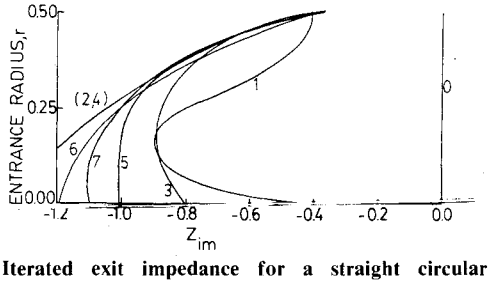

Fig. 9 Iterated exit impedance for a straight circular duct, $k = 3.1416$.

FEM calculation an impedance $Z = 1.0$ is assumed along surface 5. For the FEM calculations the inner region is divided into 200 linear triangular elements with 231 nodal points. For computations in the exterior region utilizing the integral technique, the surfaces 1 and 6 are subdivided into a total of 40 segments. Surface 1 is a hard wall and, as previously described, acoustic potentials obtained from the FEM calculations are prescribed along surface 6. The successive substitution procedure described in the preceding section is employed until the impedance of the entrance plane does not vary significantly between iterations.

The convergence for this problem is not as rapid as that found in previous examples. In this case five iterations were required to obtain a satisfactory degree of convergence. Subsequent experience has shown that the rate of convergence is somewhat dependent on the accuracy of the solution procedures. Since 40 segments represent a somewhat crude subdivision of the exterior surface, it is expected that a refinement of the segmentation will provide more rapid convergence. Figures 8 and 9 show the real and imaginary parts of the impedance at the interface after each iteration for frequencies of $k = 2.0$ and 3.146. It should be noted that at the

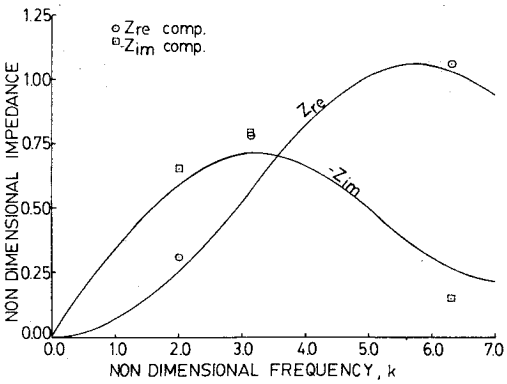

Fig. 10 Variation of mean exit impedance with frequency for a straight circular duct.

midpoint of the duct ($z=d_0/2$) where the scattering from the exit lip is reduced, the impedance across the duct is nearly uniform.

The accuracy of these computations cannot be established since there is no exact analytical solution for this problem. The exit impedances can be compared with the classical results of Levine and Schwinger[20] for plane wave propagation in a semi-infinite unflanged duct. Since this paper considers ducts of finite length, exact agreement is not expected.

Figure 10 shows the variation of the entrance plane acoustic impedance with frequency for an unflanged duct. The "classical" results for a semi-infinite duct are taken from Ref. 21. An average value of the impedance was obtained from the FEM-integral technique results using the area average

$$Z_1 \int_0^{1/2} r\,dr = \int_0^{1/2} Z_1 r\,dr \tag{23}$$

As previously stated, an exact comparison is not expected since the computed results consider a finite length duct. The results do appear to be reasonable and exhibit the correct trends. Limits on the available mass storage capacity of the Cyber 70/74 prevent calculations for longer ducts where more definitive conclusions might be obtained.

It should be noted that the iteration procedure assures a matching of φ and $\partial\varphi/\partial n$ at discrete points on the interface. Since the finite element method uses a linear variation of the potential between points and the integral technique uses a piecewise continuous variation of the potential, a consistent matching of the tangential derivative of the potential is not obtained.

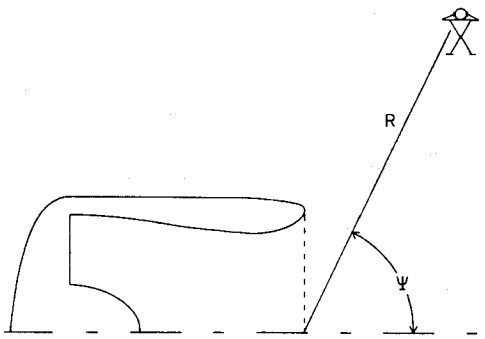

Fig. 11 Geometry of QCSEE inlet and nearfield observer.

Although this mismatching may become important when considering higher-order modes, the additional grid points required for matching the wave shape should maintain the general accuracy.

Acoustic Field of a NASA QCSEE Inlet

This final example represents the real motivation for this paper. The geometry of a NASA QCSEE inlet, shown in Fig. 11, is taken from Ref. 22. An axially symmetric wave is introduced at the inlet exit plane. All physical surfaces are taken to be hard walls. The computational procedure described in the previous section was used to obtain a continuous acoustic field. After convergence was obtained, the sound levels in the far field were computed. The variations in the sound pressure level (SPL) with respect to the angle from the inlet centerline Ψ (see Fig. 11) in the external field at $R=4d_0$ and $25d_0$ are presented in Fig. 12 for a frequency of 3.46118. Total computational time was 370 s on a CDC Cyber 70/74 computer. Also shown in Fig. 12 are the experimental results of Ref. 23. Dimensionally, the experimental data presented in Ref. 23 corresponds to a 25.4-cm-diam QCSEE inlet with the exterior measurements taken at 101.6 cm. The dimensionless frequency of 3.46118 corresponds to a 750 Hz plane wave sound source.

The comparison between the experiment and the computed results is seen to be quite good. However, Fig. 12 is somewhat misleading in that the accuracy is more dependent on the acoustic solution method used in the exterior region (i.e., the integral technique), than on the "continuity" of the acoustic field. To illustrate this fact, Table 1 compares the experimental values with the final computed values (after 5 iterations) and with the sound levels computed on the first iteration. It is seen that on the first iteration, the magnitude of the sound field is a fairly good approximation to the experimental values (about 2-dB error) while repeated iterations

Table 1 Experimental and theoretical values for SPL and phase of a NASA QCSEE inlet for a 750-Hz plane wave driver, $R=4d_0$

Degrees off centerline	Experimental SPL, dB	Experimental Phase, deg	One iteration SPL, dB	One iteration Phase, deg	Five iterations SPL, dB	Five iterations Phase, deg
0.00	109.5	−158	105.9	−135	106.0	−152
11.25	108.5	−163	105.7	−135	105.8	−152
22.50	107.2	−162	105.1	−136	105.3	−153
33.75	105.6	−166	104.3	−136	104.5	−154
45.00	105.2	−167	103.2	−137	103.4	−155
56.25	102.6	−153	101.9	−137	102.2	−156
67.50	101.2	−162	100.4	−136	100.8	−156
78.75	101.9	−154	98.9	−133	99.5	−155
90.00	99.9	−148	97.5	−130	98.1	−153
Driver	127.0	0	127.0	0	127.0	0
Absolute error			1.9	24	1.8	7

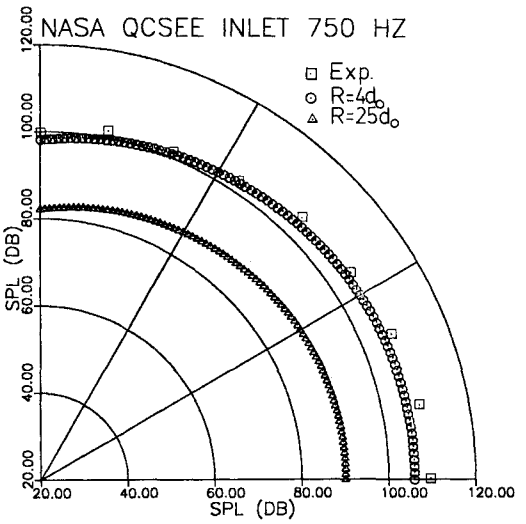

Fig. 12 Sound pressure level distribution of NASA QCSEE inlet for $k = 3.46118$.

have little effect in improving the accuracy of the sound pressure level. The real improvement is seen in the comparison of the computed pressure phase angles relative to the driver. In the first iteration, the difference in phase between the experimental values and the computed values is quite large (approximately 24 deg), while the final iterated values for a uniform acoustic field have a relatively small error (approximately 7 deg).

Additional computations have been made for frequencies of $k = 1.38447$ (300 Hz), and $k = 2.30745$ (500 Hz). In all cases, the comparison between the computed and measured sound fields (both magnitude and phase) was found to be excellent.

Conclusions

The problem of sound propagation in ducts and subsequent radiation to the external environment has been considered. The acoustic field is divided into a finite interior region and an infinite exterior region. An iterative procedure is presented which forces the interior and exterior regions to match at the interface, thus producing a continuous acoustic field. A finite element method is utilized to obtain solutions in the interior region and an integral technique is applied to the external region, although other appropriate computational schemes could be employed.

Convergence to a uniform acoustic field was obtained for all cases considered, i.e., the solutions for the interior and exterior regions "matched" at the interface. This result confirms the arguments of Baumeister that iterations between the regions should be convergent. For problems with simple geometries, convergence is obtained in approximately two or three iterations. Only five iterations were required for the most complex problem tested (QCSEE inlet). More sophisticated iteration techniques could be developed to speed convergence for these complex problems if deemed necessary.

Computational results are presented for a number of acoustic problems ranging from simple mathematical models, i.e., an oscillating sphere, to the physical problem of sound propagation from a QCSEE inlet. Comparison of the computed results with exact solutions and experimental results, respectively, show very good agreement. These results are encouraging and support the belief that an iterative scheme can be developed that will have the capability of predicting the entire sound field of a "real world" turbofan inlet.

The next step in the development of a computational procedure for predicting the continuous acoustic field of a turbofan inlet is the consideration of steady flows. Efforts to extend this approach to inlets with steady flows is currently in progress and preliminary results are highly encouraging.

Acknowledgments

This research was sponsored by NASA Lewis Research Center under Grant NSG 3036. The authors would like to express their appreciation to Dr. Kenneth J. Baumeister for his support and advice.

References

[1] Tyler, J. M and Sofrin, T. G., "Axial Flow Compressor Noise Studies," *SAE Transactions*, Vol. 70, Society of Automotive Engineers, New York, N.Y., 1962, pp. 309-332.

[2] Rice, E. W., "Attenuation of Sound in Soft-Walled Circular Ducts," *Aerodynamic Noise*, edited by H. S. Ribner, Univ. of Toronto Press, 1969, pp. 229-249.

[3] Tag, I. and Lumsdaine, E., "An Efficient Finite Element Technique for Sound Propagation in Axisymmetric Hard Wall Ducts Carrying High Subsonic Mach Number Flows," AIAA Paper 78-1154, 1978.

[4] Lumsdaine, E., "Calculation of Pressure Reflection Ratio," *Journal of Sound and Vibration*, Vol. 52, No. 1, 1977, pp. 145-148.

[5] Baumeister, K. J., "Numerical Spatial Marching Techniques in Duct Acoustics," *Journal of the Acoustical Society of America*, Vol. 65, Feb. 1979, pp. 297-306.

[6] Sigman, R. K., Majjigi, R. K., and Zinn, B. T., "Use of Finite Element Techniques in Turbofan Inlets," *AIAA Journal*, Vol. 16, Nov. 1978, pp. 1139-1145.

[7] Majjigi, R. K., Sigman, R. K., and Zinn, B. T., "Wave Propagation in Ducts Using the Finite Element Method," AIAA Paper 79-0659, March 1979.

[8] Abrahamson, A. L., "A Finite Element Algorithm for Sound Propagation in Axisymmetric Ducts Containing Mean Flow," AIAA Paper 77-1301, Oct. 1977.

[9] Baumeister, K. J. and Bittner, E. C., "Numerical Simulation of Noise Propagation in Jet Engine Ducts," NASA TN D-7339, 1973.

[10] Quinn, D. W., "A Finite Difference Method for Computing Sound Propagation in Non Uniform Ducts," AIAA Paper 75-130, 1975; also *AIAA Journal*, Vol. 13, Oct. 1975, pp. 1392-1393.

[11] Nayfeh, A. H., Shaker, B. S., and Kaiser, J. E., "Transmission of Sound Through Nonuniform Circular Ducts with Compressible Mean Flows," *AIAA Journal*, Vol. 18, May 1980, pp. 515-525.

[12] Eversman, W., Astley, R. J., and Thanh, V. P., "Transmission in Nonuniform Ducts—A Comparative Evaluation of Finite Element and Weighted Residuals Computational Schemes," AIAA Paper 77-1299, Oct. 1977.

[13] Meyer, W. L., Bell, W. A., Stallybrass, M. P., and Zinn, B. T., "Prediction of the Sound Field Radiated from Axisymmetric Surfaces," *Journal of the Acoustical Society of America*, Vol. 65, March 1979, pp. 631-638.

[14] Bell, W. A., Meyer, W. L., and Zinn, B. T., "Predicting the Acoustics of Arbitrarily Shaped Bodies Using an Integral Approach," *AIAA Journal*, Vol. 15, June 1977, pp. 813-820.

[15] Hess, J. L., "Calculation of Acoustic Fields about Arbitrary Three-Dimensional Bodies by a Method of Surface Source Distributions Based on Certain Wave Number Expansions," Douglas Aircraft Co., Rept. DAC 66901, March 1968.

[16] Sigman, R. K., Majjigi, R. K., and Zinn, B. T., "Use of Finite Element Techniques in the Determination of the Acoustic Properties of Turbofan Inlets," AIAA Paper 77-18, Jan. 1977.

[17] Meyer, W. L., Bell, W. A., Zinn, B. T., and Stallybrass, M. P., "Boundary Integral Solutions of Three-Dimensional Acoustic Radiation Problems," *Journal of Sound and Vibration*, Vol. 59, No. 2, 1978, pp. 245-262.

[18] Zienkiewicz, O. C., Kelley, D. W., and Bettess, P., "The Coupling of the Finite Element Method and Boundary Solution Procedures," *International Journal for Numerical Methods in Engineering*, Vol. 11, No. 2, 1977, pp. 355-375.

[19] Zienkiewicz, O. C. and Chung, Y. K., *The Finite Element Method in Continuous Structural Mechanics*, McGraw-Hill, New York, 1967.

[20] Levine, H. and Schwinger, J., "On the Radiation of Sound from an Unflanged Circular Pipe," *Physical Review*, Vol. 73, Feb. 1948, pp. 383-406.

[21] Morse, P. M. and Ingard, K. V., *Theoretical Acoustics*, McGraw-Hill, New York, 1968.

[22] Miller, B. A., Dastoli, B. J., and Wesoky, H. L., "Effect of Entry-Lip Design on Aerodynamics and Acoustics of High-Throat-Mach-Number Inlets for the Quiet, Clean, Short-Haul Experimental Engine," NASA TM X-3222, May 1975.

[23] Zinn, B. T., Meyer, W. L., and Daniel, B. R., "Noise Suppression in Jet Inlets," AFOSR-TR-80-0452, Feb. 1980.